Imaging the Interaction Region of Heavy-Ion Collisions

Cade Rodgers
Advisor: Daniel Cebra
Department of Physics, The University of California at Davis
(Dated: August 19, 2022)

The interaction region of heavy-ion collisions, a term referred to as the "fireball", is an important probe for both the high and low energy scales of Quantum Chromodynamics. Thus, it important to study the structure of this fireball at various energies. Here we present a method for determining the three dimensional shape and size of this fireball. The model exploits information regarding the transverse mass distribution of pions created thermally from the fireball to determine the electric potential of the fireball, which can be converted into a distance by using both Gauss's law and an assumption on the distribution of protons within the volume. Looking at this distance as a function of rapidity allows us to generate a two dimensional image of the fireball, which combines with the symmetry of our system to produce a full three-dimensional model of the fireball. We find the fireball to be approximately spherical in shape, with the size in the longitudinal direction being $a = 5.95 \pm 0.13$ fm and the maximum size in the transverse plane being $b = 6.15 \pm 0.24$ fm. This result agrees with a previous study that was conducted, which used a different method than the one we employed here.

I. INTRODUCTION

A. Background

The field of nuclear physics is primarily based around treating nucleons (ie, protons and neutrons) as the relevant degrees of freedom to study things like nuclear structure, reaction cross-sections, and radioactive decay (amongst many other things within the field). However, quarks and gluons are what comprise nucleons, and thus are important objects to study to gain a deeper understanding of nuclear physics. Quarks, gluons, and their interactions are governed by Quantum Chromodynamics (QCD). QCD is a strongly interacting field theory, meaning its properties become challenging to study at low energies/large length scales. As this is the regime that most particles are subject to in nature, it is difficult to make precise calculations and predictions about particles using QCD, resulting in the need for powerful supercomputers and nonphysical assumptions (such as the mass of the pion) to calculate something as simple as the proton's mass. Conversely, at higher energies the terms that cause QCD to be so challenging in the low energy regime become negligible, allowing the use of perturbative methods that allow for a more effective study of the interactions governed by the theory.

It is precisely because of this dependence on energy that the interaction region of heavy ion collisions, a term we often refer to as the "fireball", serves as a way to test the accuracy of our various models within QCD. A high temperature/low baryon chemical potential fireball (corresponding to high energy particle collisions) occurs in the high energy regime of QCD, allowing us to test theoretical predictions of the fireball's properties and structure made by perturbative methods of QCD against experimental data. In turn, we can use the data from particle collisions resulting in a low temperature/high baryon chemical potential fireball (corresponding to the low energy regime of the QCD energy scale) to extend our knowledge of QCD in this non-perturbative region. Thus, to gain a better understanding of QCD, which in turn will give us a deeper understanding of nuclear physics as a whole, it is important to map out the structure of the collision interaction region experimentally in this low-energy regime.

B. Project Overview

As part of this effort, the data focused on throughout this paper is from $\sqrt{s_{NN}} = 4.5$ GeV $Au + Au$ collisions at the STAR Fixed Target (FXT) experiment at Brookhaven National Laboratory. This experiment run is part of a larger effort to study the QCD phase diagram, an effort known as the Beam Energy Scan program (BES). The analyzed energy corresponds to a low-temperature fireball resulting from the collisions, thus placing it in the low energy regime of QCD. This low energy was attained by firing a beam of ionized gold atoms at a fixed gold target positioned inside of the Relativistic Heavy Ion Collider (RHIC) at BNL, rather than colliding two separate beams of gold ions. This Fixed-Target method was proposed and implemented by UC Davis's Daniel Cebra. A schematic of the STAR detector can be seen in Figure 1, highlighting the coordinate system that will be used throughout the entirety of this analysis: z being the direction along the fired gold beam (this will also be referred to as the longitudinal direction), with the xy-plane being orthogonal to the beam's direction (this will be referred to as the transverse plane). The analysis of the data is primarily focused on determining the spatial distribution of the "fireball". Specifically, we are interested in the distribution of the fireball at a point known as "chemical freeze-out". Chemical freeze-out occurs when the fireball has expanded and cooled to the point that particles are no longer being thermally

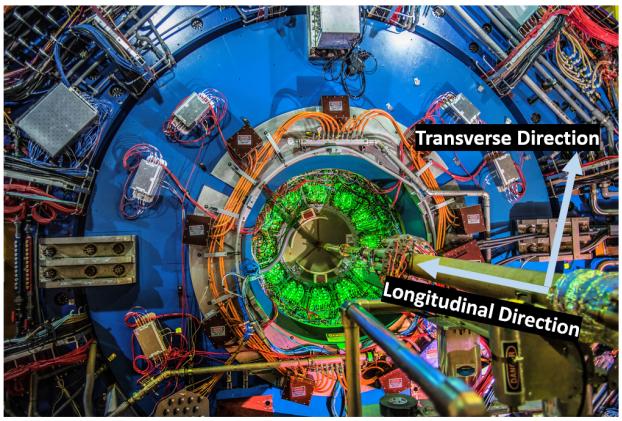

FIG. 1: The STAR detector with the coordinate system we have defined superimposed. Note that the transverse direction is a plane, as there is a component that points "out of the page" that is not shown.

created, leaving the number of hadrons after this point fixed. This point is when we consider the fireball to have dissipated, making the spatial distribution at chemical freeze-out a probe of the fireball's final state behavior. Further, we are also attempting to compare the shape of the fireball obtained from our method to an interferometry method employed in Reference [1], which was performed at the same energy.
It should be noted that the 4.5 GeV energy used in this analysis was previously analyzed by former UC Davis graduate student Dr. Kathryn Meehan [2]. The present analysis will utilize data that contains 10 times more statistics than the work presented by Kathryn. Further, the particle identification methods of STAR, as well as the analysis methods used by the UC Davis team, have been improved since Kathryn's work.

C. Organization of Paper

The first step in the analysis was converting the raw data files obtained from the experiment run into data that could be utilized for analysis. Section II contains an overview of how this was done, with the process ultimately resulting in ROOT files containing the number of particles detected in the experiment run, separated by particle species, rapidity (all of which will be reported in the center-of-mass frame), and transverse mass. From this data we were able to conduct our analysis, the steps of which are detailed in Section III. The results of our analysis, as well as a comparison of our result against the aforementioned interferometry method, are presented in Section IV. Finally, Section V contains concluding remarks, as well as a brief discussion.

II. DATA COLLECTION

A. Centrality Determination

In heavy-ion collisions, the spatial distribution of nucleons within the ions results in a variable number of nucleon-nucleon interactions occurring upon collision. The more nucleon-nucleon interactions that occur in a given collision, the more energy is distributed into the resulting fireball, which leads to a greater number of particles created. Thus, measuring the number of particles created by a collision, a quantity we refer to as "multiplicity", gives us insight into the number of interactions that occurred. The multiplicity is directly related to how central the collision between the two ions was, as head-on collisions result in more interactions than if the two ions glance off each other, or miss entirely. For this reason, we characterize collisions by their centrality, where a centrality class of $0-5\%$ corresponds to the most central collisions (ie, highest multiplicity), and so on. As collision centrality leads to increased size in the fireball (due to more interactions contributing to its size), to get an accurate comparison of the fireball's size we need to choose events that belong to the same centrality class.
To obtain centrality classes, we first need to determine the multiplicity distribution of the collision data. While multiplicity is a measured observable, we have to account for a phenomenon called "pile-up", which occurs when the particles from different collisions are treated as having come from the same event by the vertexing algorithm. To account for this pile-up effect we performed a fitting routine that utilized a Monte-Carlo Glauber model, which simulated the ion collisions and generated an artificial multiplicity distribution. The number of nucleon+nucleon interactions for a given collision is assumed to follow a negative binomial distribution, while the nucleons themselves are assumed to be distributed within the nucleus in accordance with a Woods-Saxon distribution. The Glauber model used by the UC Davis group incorporates the "hardness" of the collisions, x, the average number of particles produced in proton+proton interactions (ie, how many particles are expected per nucleon+nucleon interaction), n_{pp}, and a shaping parameter k of the negative binomial distribution as parameters in their fit. We also expect the detector's efficiency to have a dependence on energy, an effect that produces an efficiency curve. Thus, for the model to accurately match the measured data it is useful to incorporate detector inefficiency into the model. As these efficiency curves aren't easily attained quantities, I modified the Glauber model so that it treated the detector inefficiency as a free parameter to be fit, with this change being incorporated into a UC Davis repository "glaubermchardness", which is used for centrality determination. After incorporating the detector efficiency into the Glauber model, the simulation was ran, generating the multiplicity distribution shown in Figure 2. From this distribution we were able to classify the data by centrality, which was done by as-

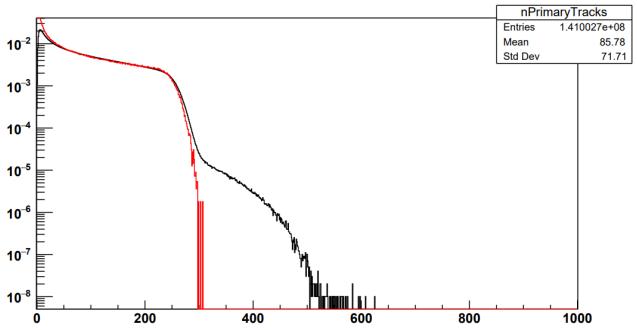

FIG. 2: This figure depicts the multiplicity distribution of our collision events, with the x-axis corresponding to multiplicity and the y-axis being the (normalized) number of collisions. The red line is our Glauber model fit, with the divergence of our fit to the data at high multiplicity being a result of pile-up. Centrality is determined by integrating the fit such that each centrality bin contains an equal number of counts.

sociating each centrality bin with 5% of the total number of collision counts, with the multiplicity cuts for each bin being given in accordance with Table I. Throughout the entirety of this analysis, only the 0-5% centrality bin was considered.

TABLE I: Centrality bins and their associated multiplicity cut-off. A centrality of $0-5\%$ corresponds to the most central events, thus it is associated with the highest multiplicity events. Conversely, $75-80\%$ are the least central events and thus represent events with the lowest multiplicity. Each centrality bin represents 5% of the total counts of the integrated Glauber fit. For our analysis only events with a centrality in the $0-5\%$ range were used.

Centrality	Multiplicity cutoff
$75-80\%$	5.50
$70-75\%$	7.50
$65-70\%$	10.50
$60-65\%$	14.50
$55-60\%$	19.50
$50-55\%$	25.50
$45-50\%$	33.50
$40-45\%$	43.50
$35-40\%$	55.50
$30-35\%$	69.50
$25-30\%$	86.50
$20-25\%$	105.50
$15-20\%$	128.50
$10-15\%$	154.50
$5-10\%$	184.50
$0-5\%$	218.50

B. Uncorrected Raw Spectra

The result of the centrality cut procedure discussed in Section II A was a file that was incorporated into a UC Davis software called ZFitter, which is contained in the repository "lightflavorspectra_etof". This software performed hundreds of fits on the data obtained from the experiment run, resulting in the particle yield of protons, pions, and kaons (as well as their associated antiparticles). The yields of each particle species were given as a function of the particle's rapidity in the longitudinal direction (i.e, $\beta_z = v_z/c = \tanh(y)$, where y is the rapidity in the center-of-mass frame), as well as the transverse mass of the particle (defined by $m_T = \sqrt{m^2 + p_T^2}$, where m is the rest mass of the particle, and $p_T^2 = p_x^2 + p_y^2$ is the momentum of the particle in the transverse plane). This was done as these two quantities, rapidity and m_T, are utilized in the particle identification process, which is outlined in Dr. Meehan's thesis [2]. The largest issue faced with this procedure was the influence of other particle species on these yields, caused by the merging of the "particle bands" used for particle identification, as described in Section 2 of Reference [2]. To address this issue, I developed a background model that treated the influence of other particle species as a decaying exponential function (in log-space), when such a merging occurred (otherwise, no background model is needed). An example of this background model and overall fitting process is seen in Figure 3, with this representing measured K^+ (positive kaons) with background influence from π^+ (positive pions) on the left-hand side. The particle yields obtained from ZFitter that were relevant for the present analysis were the yields of π^+, π^-, and p across all rapidities and m_T.

III. METHODS

A. Coulomb Potential

Due to the fireball having a net positive charge, which results from the large number of protons that are present during the collision, there is an effect on the m_T distribution of π^+ (which are repelled by the positive charge and thus sped up) and π^- (which are attracted to the fireball and thus slowed down). Using the particle yields obtained from ZFitter, we can look at how the ratio of π^+ to π^- changes as a function of $m_T - m_\pi$ for a given rapidity, expecting to see more π^- with a low m_T than π^+. More information of this phenomenon can be found in References [3][4], with an example of this effect being shown in Figure 4.

From this information, we can extract the electric Coulomb potential of the fireball using the equation [3]

$$R_f(E_f) = \frac{E_f - V_c}{E_f + V_c}\frac{\sqrt{(E_f + V_c)^2 - m^2}}{\sqrt{(E_f - V_c)^2 - m^2}}\frac{n^+(E_f - V_c)}{n^-(E_f + V_c)} \tag{1}$$

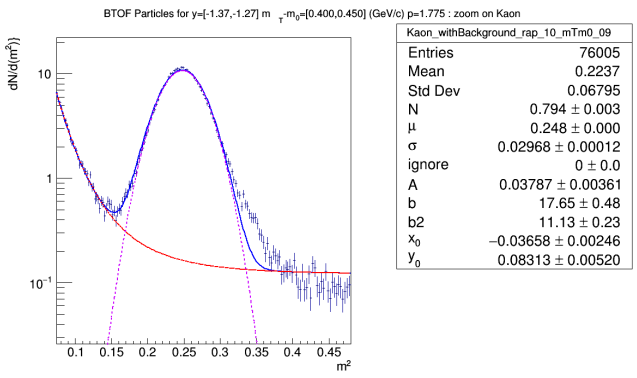

FIG. 3: An example of the fitting procedure performed by ZFitter, where the blue curve represents the distribution of kaons in a rapidity range of $y = [-1.37, -1.27]$ and a transverse mass bin of $m_T - m_0 = [0.4, 0.45]$, which we assume to be Gaussian in log-space (the pure Gaussian is depicted in purple). The red curve represents a fit on the background contribution of pions, which is a decaying exponential in log-space. The table to the right of the figure contains the results of our kaon distribution fit, which has parameters N, μ, and σ, as well as our background fit. Integrating the kaon distribution gives us the yield of kaons for this particular rapidity and transverse mass range.

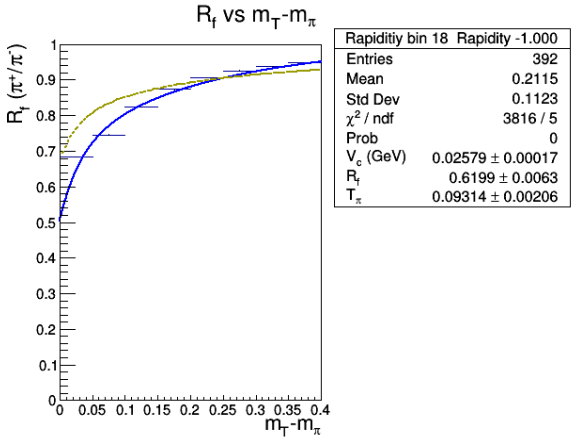

FIG. 4: A representative example of the fireball's Coulomb effect on the transverse momentum distributions of π^+ versus π^-. The y-axis represents the ratio π^+/π^- as a function of transverse mass on the x-axis, thus we see that we have significantly more π^- with low $m_T - m_\pi$ than π^+, which is expected due to the attractive/repulsive Coulomb effect. As seen, this effect is greatest at low momenta (ie, low $m_T - m_\pi$), due to the magnitude of the Coulomb effect being small and thus most noticeable for low momenta particles. The blue curve is a result of fitting Equation 1 to this data, with the dashed yellow curve representing our initial seed.

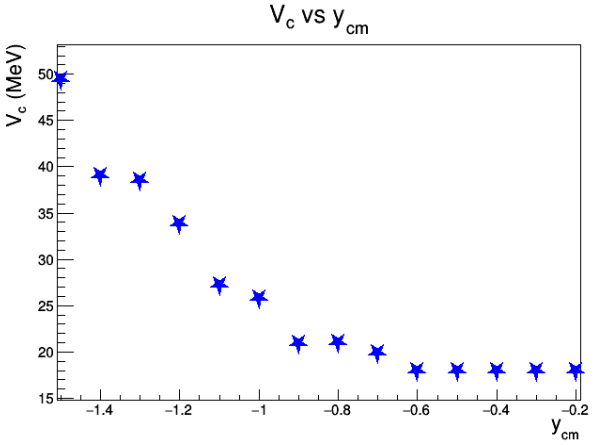

FIG. 5: The Coulomb potential of the fireball as a function of rapidity. There is a clear downward trend as rapidity goes to zero, which corresponds to distances close to the collision target. All rapidities displayed are negative, indicating that these particles moved backwards from the target upon collision (ie, negative z-direction). The detector geometry prevented good statistics for rapidities at mid-rapidity ($y = 0$) and beyond, hence no data is present for the potential at these rapidity values.

where $R_f(E_f)$ is the observed ratio of π^+ to π^- as a function of the final energy $E_f = m_T \cosh(y)$, V_c is the Coulomb potential of the fireball (our quantity of interest), and $n^+(E_f - V_c)/n^-(E_f + V_c)$ is the emission function that resulted in the initial pion distribution. This is taken to be a Bose-Einstein distrubtion, thus

$$\frac{n^+(E_f - V_c)}{n^-(E_f + V_c)} = R_i \frac{e^{(E_f + V_c)/T_\pi} - 1}{e^{(E_f - V_c)/T_\pi} - 1}, \tag{2}$$

where here we have R_i being the initial ratio of the pions when they were thermally created in the fireball (prior to any repulsive/attractive effects of the fireball itself), and T_π is the slope parameter of the pion's Bose-Einstein distribution.

Fitting our pion ratio data to Equation 1 thus gives us V_c for a given rapidity, where we also treated T_π and R_i as parameters to be fit, with initial seed values being obtained from Reference [3]. A result of this fitting procedure is displayed in Figure 5 As the statistics of our pion ratio data was low for rapidities larger than $y = -0.2$, only V_c for data in the rapidity range $-1.5 \leq y \leq -0.2$ (where -1.5 is the rapidity of our target in the center-of-mass frame, a term we'll refer to as "target rapidity") was used for the rest of the analysis, in increments of 0.1. Doing this fitting procedure across all rapidities within this range thus tells us how the potential of the fireball changes with respect to rapidity, which is highlighted in Figure 5.

B. Transverse Distance

The data contained in Figure 5 shows a potential versus rapidity – however, we are interested in mapping out the spatial distribution of the fireball, meaning we need to convert these quantities to a distance. This section is dedicated to converting the Coulomb potential of the fireball into a distance in the transverse plane. Due to the azithumal symmetry of the fireball, this tells us the full shape of the fireball in this plane.
To convert potential to a distance we use a simple spherical model to which we can apply Gauss's law, yielding [5]

$$V_c = \frac{6}{5}\frac{e^2}{4\pi\epsilon_0}\frac{Z_{part}}{R}, \tag{3}$$

where Z_{part} is the charge contained in our Gaussian sphere, which we are assuming arises from uniformly distributed protons, and R is the size of the sphere at a given rapidity. R is our quantity of interest, as the radius of the sphere tells us the size of the fireball in the transverse plane, since we are looking at data for a given rapidity which fixes our longitudinal distance. Solving Equation 3 for R and using results from a former UC Davis student Samantha Brovko to obtain Z_{part} as a function of rapidity, we can compute the size of the fireball in the transverse plane and plot it against rapidity, which is presented in Figure 6. It should be noted that the data used to compute Z_{part} only contained information for $-1.3 \leq y \leq -0.2$, thus a fit was used to extend the data to target rapidity ($y = -1.5$). These extrapolated points contained no systematic uncertainties, resulting in much smaller error bars compared to the measured data, as seen in Figure 6.

C. Longitudinal Distance

Having found the size of the fireball in the transverse plane in Section III B, we must now convert rapidity into a distance. As our measured rapidities correspond to the rapidity of the particles in the z-direction, this will correspond to a distance in the longitudinal direction along the beam. A simple calculation using the definition of rapidity tells us that the longitudinal distance is $t \cdot \tanh(y)$, where t is the lifetime of the fireball. We can estimate t using the results of the interferometry study [1] to be $t = 6.84$ fm/c. This was found by taking the measured longitudinal distance found in Reference [1] (averaged across all rapidities), which is 4.2 fm, and dividing by the average longitudinal velocity of the pions from our data. With this we can now convert our rapidities into a longitudinal distance, thus giving us a full spatial description of the fireball in the transverse and longitudinal directions. This is shown in Figure 7a.

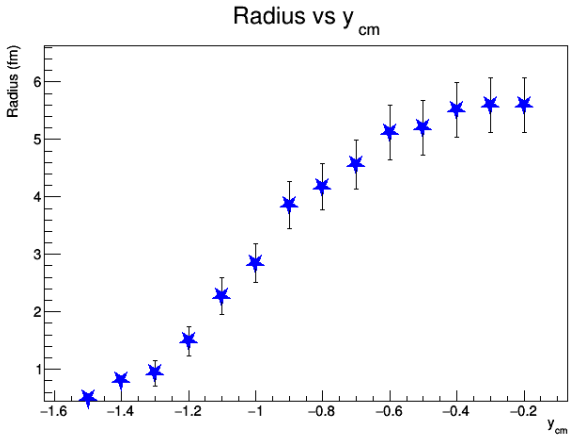

FIG. 6: The radius of the fireball plotted against rapidity, calculated using Equation 3. As this radius is calculated for a given rapidity (corresponding to a given distance in the longitudinal direction), it corresponds to the size of the fireball in the transverse plane. The points at $y = -1.4$ and $y = -1.5$ were calculated using Z_{part} information obtained from a fit, thus the uncertainties associated with these points are much lower than the uncertainties for the other data points, as they don't account for the systematic uncertainty that's present in these other data points.

IV. RESULTS

The data shown in Figure 7a contains the shape of the fireball at negative distances from the target's location (ie, behind the target). Assuming symmetry with respect to rapidity (and thus longitudinal distance), this same shape holds for the region of the fireball in front of the target, allowing us to fit Figure 6 for an ellipse and extrapolate this to the first quadrant, resulting in Figure 7b. Exploiting azimuthal symmetry then allows us to view this image as a three-dimensional ellipsoid with semi-minor/major axes $a = 5.95 \pm 0.13$ fm and $b = 6.15 \pm 0.24$ fm respectively, where b corresponds to the major axis in both transverse directions, and a is the size of the fireball along the beam axis. The full three-dimensional shape can be seen in Figure 8. The uncertainties reported here reflect both statistical and systematic uncertainties, which were calculated using the quadrature method to propagate the uncertainty of both our various fit results and our Z_{part} and pion ratio data.
The interferometry method of Reference [1] yielded a semi-minor/major axis of 4.2 ± 0.3 fm and 4.5 ± 0.3 fm, respectively. Figure 9 shows where the results we computed in our analysis correspond with those from [1], as well as various other analyses at different collision energies.

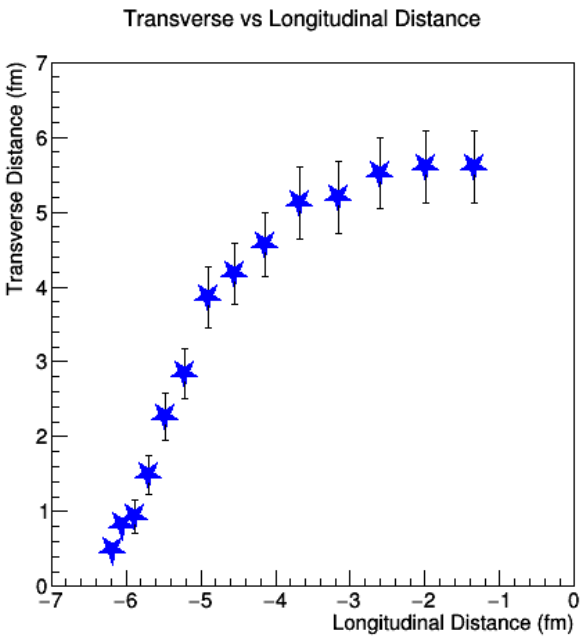

(a) The result of converting our rapidities to a longitudinal distance and plotting it against the transverse distances computed using Equation 3

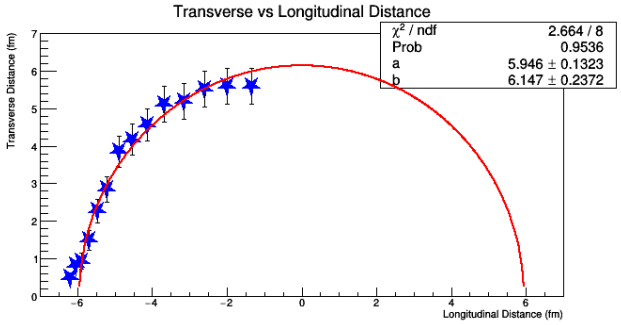

(b) The data from (a) after being fit with an ellipse and extrapolated to the positive z-axis. The semi-major and semi-minor axes are displayed in the statbox, where "a" corresponds to the size of the fireball in the longitudinal direction and "b" is the size in the transverse plane.

FIG. 7: The two dimensional shape of the fireball. The top figure, (a), shows the raw data, which was then fitted with an ellipse to obtain the shape of the fireball both forward and behind the collision target, which is shown in the bottom figure, (b). Using azimuthal symmetry allows us to convert these images to a full three-dimensional depiciton of the fireball's shape

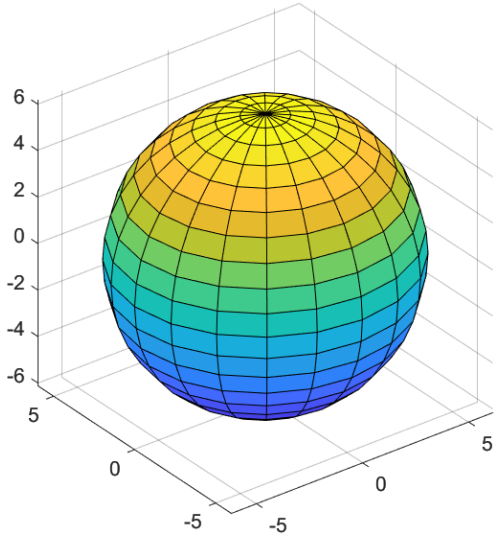

(a)

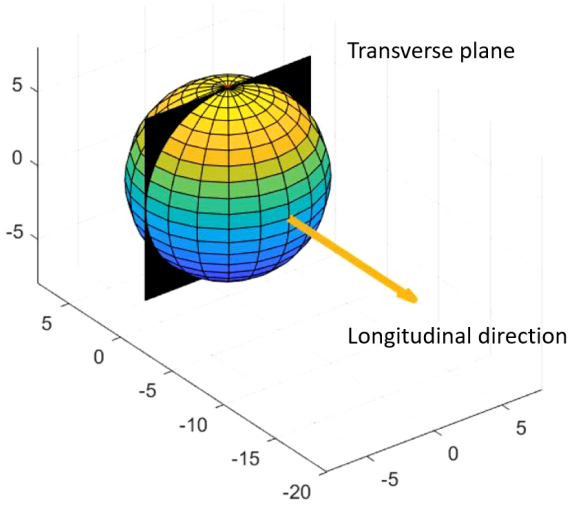

(b)

FIG. 8: The three dimensional shape of the fireball. The top figure, (a), shows the full spatial distribution of the fireball, with the bottom figure, (b), providing visual aids to see how the fireball is oriented with respect to the displayed coordinate system.

V. CONCLUSION

A. Discussion

The results reported in Section IV for our analysis method differ by several standard deviations from those reported by Reference [1]. However, the interferometry method differed from our analysis in two important ways: 1) they averaged their distances across all rapidities, which would naturally lead to a reduced longitudinal distance when compared to our method, and 2) they calculated the size of the "region of homogeneity" of the fireball, a quantity described in terms of two-particle correlations, whereas our analysis measured the size of the fireball at chemical freezeout. Both of these differences would be expected to result in a reduced "size" of the fireball when compared to our method, which is what we observe when comparing the two results. It is the

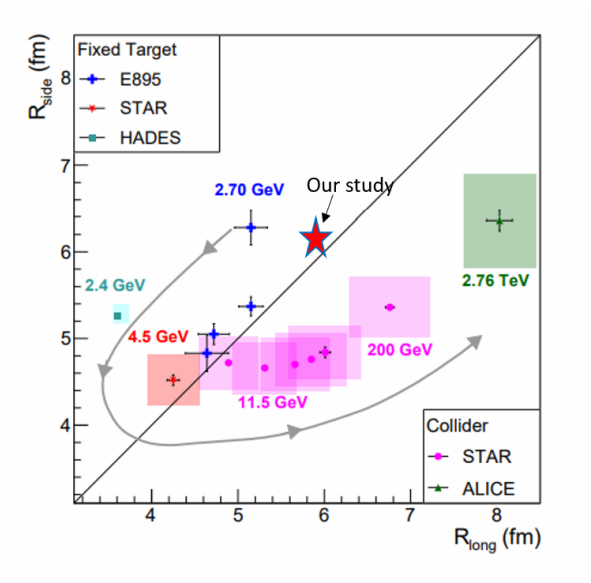

FIG. 9: The result of the interferometry method used by Reference [1] is displayed as the red square associated with 4.5 GeV, and is shown amongst other studies of the fireball's size at different energies. The x-axis, labeled here as R_{long}, corresponds to the longitudinal size of the fireball, while R_{side} is the size in the transverse plane. The result we obtained using the Coulomb method is superimposed on the figure, being represented by the red star. Note both the interferometry method and our method predict a roughly spherical shape for the fireball, where the line running through the middle of the figure corresponds to a spherical shape

general shape of the fireball that we expect to remain consistent between the two methods. The interferometry method reports the fireball as being roughly spherical at $\sqrt{s_{NN}} = 4.5\,\text{GeV}$, with a maximum eccentricity of approximately $\epsilon \approx .35$. This is precisely the result that we obtain from our presented Coulomb method, which suggests that the model presented in our analysis agrees with the interferometry method regarding the shape of the interaction region, at least for the most central collisions (as these are the ones studied in both analyses).

We did assume that the distribution of protons within the fireball was uniform, where a more accurate distribution would be that of 3D Gaussian profile. However, this assumption allows for simplified calculations and results in transverse radii that deviate from those calculated assuming a Gaussian distribution only marginally with respect to the systematic/statistical uncertainty [5].

B. Concluding Thoughts

We devised a method to determine the three-dimensional shape of the interaction region of heavy-ion collisions. The model used information regarding the momentum distribution of pions to calculate the transverse size of the collision fireball, and combined the time of chemical freeze-out with rapidity to determine the size of the fireball in the longitudinal direction. This model, which made assumptions regarding the charge distribution of the fireball and used non-relativistic electromagnetic equations to calculate the distances, resulted in a shape that agreed with a previous study which used a different method at the same energy [1], with both methods predicting a roughly spherical shape.

[1] Jaroslav Adam et al. Flow and interferometry results from Au+Au collisions at $\sqrt{s_{NN}} = 4.5$ GeV. *Phys. Rev. C*, 103(3):034908, 2021.
[2] Kathryn Meehan. Pion Production in 4.5 GeV Au + Au Collisions from the STAR Fixed-Target Pilot Run. 2018.
[3] Dan Cebra et al. Coulomb effect in Au+Au and Pb+Pb collisions as a function of collision energy. 2014.
[4] B. A. Haag et al. Coulomb effect in $Au_{like} + Al$ collisions at $\sqrt{s_{NN}} = 3.0$, 3.5, and 4.5 GeV.
[5] J. Adamczewski-Musch et al. Impact of the Coulomb field on charged-pion spectra in few-GeV heavy-ion collisions. 2022.